

An Investigation of LENS®-Deposited Medical-Grade CoCrMo Alloys

Brent Stucker*, Carson Esplin**, and Daniel Justin**

* Mechanical & Aerospace Engineering, Utah State University, Logan, UT 84322-4130

** MedicineLodge, Inc., 180 South 600 West, Logan, UT 84321

Reviewed, accepted August 4, 2004

ABSTRACT

A series of deposition experiments using CoCrMo were performed using an Optomec LENS®¹ machine. An analysis of hardness, microstructure, and wear trends of the deposited alloys was undertaken in an attempt to determine the applicability of using LENS® to create better materials for orthopedic implants. It was found that LENS®-deposited CoCrMo alloys were harder than wrought materials, however initial wear tests indicated that LENS®-deposited alloys were less resistant to abrasive wear than wrought alloys.

INTRODUCTION

Many knee and hip total joint replacements performed in the United States use polyethylene-on-CoCrMo bearing surfaces due to the forgiving nature of the combination to the individual biomechanical nuances of joint recipients. Current studies show that, although polyethylene is biologically inert in the body as a whole, microscopic particles of polyethylene that result from years of wear can possibly be toxic if encountered in large amounts and lead to osteolysis (Ratner et al. 1996; Amstutz et al. 1992; Hamilton and Gorczyca 1995). This has led to a growing interest in metal-on-metal bearing surfaces for implants (Walker and Gold 1971; Medley et al. 1996). A number of metal-on-metal hip implants survived more than 25 years with low wear rates and minimal osteolysis (Schmalzried et al. 1996). Surgeons will likely prefer metal-on-metal joints over polyethylene-on-metal when scientists can mitigate the causes for early failure of metal-on-metal implants.

Cobalt-based alloys are frequently used in applications that require wear and/or corrosion resistance. CoCrMo is the hardest known biocompatible metal alloy. This makes it an ideal candidate for metal-on-metal bearing surfaces in orthopedic implants. Several microstructural characteristics determine the material properties and thus the life of a CoCrMo implant. First, a finer grain size can contribute to higher tensile strengths and improved fatigue strengths. Second, carbide precipitates are the main contributors to the wear protection for metal-on-metal interfaces. Carbide volume fraction, shape, morphology, and the strength of the carbide/matrix interface play a significant role in determining the amount of wear resistance of a particular alloy (Steen 1985).

Laser Engineered Net Shaping™ (LENS®), a technology commercialized in the 1990s, allows for microstructural control during part fabrication. The LENS® process melts a powdered metal onto a substrate using a high-powered laser and has the advantage of directly controlling the heating properties within a localized area, thus affecting the grain structure and morphology.

The LENS® process can control several parameters that affect cooling rate, which alter the microstructure of a deposited material. Recent research has focused mainly on the effect of laser power and laser traverse speed on microstructure (Hofmeister et al. 2001; Kobryn et al. 2000). In addition, other parameters such as powder feed rate, hatch spacing, and layer thickness

¹ LENS® is the registered trademark and service mark of Sandia National Laboratories and Sandia Corporation.

affect the porosity, which can directly alter material strength (Brice et al. 1999; Kobryn and Semiatin 2001).

EXPERIMENTAL PROCEDURES

The scope of these experiments was designed to determine the feasibility of depositing medical grade CoCrMo with the LENS® process, then to investigate the hardness, microstructure, and wear properties when compared to wrought CoCrMo to develop a foundation for future CoCrMo/LENS® work.

The experimental procedure comprised three phases. The first phase was a full factorial experiment looking at the relationship between LENS® parameter variations and the resultant microstructure and hardness. Phase 2 was a verification of the 16 best parameter combinations from Phase 1. Phase 3 examined the wear properties of LENS®-deposited materials versus wrought materials.

Carpenter Technologies Biodur CCM+ alloys were used in these experiments. This included both the substrate and the powdered metal. Quarter-inch thick disks cut from 2.25-inch diameter wrought bar stock, produced according to ASTM F 1537, formed the substrate. The powdered metal had an identical elemental composition but was formed using gas atomization with powder sifted to a -100/+325 mesh size. Table 1 shows the composition of the material.

Table 1. Biodur CCM+ Composition

| Element | wt% | Element | wt% | Element | wt% |
|----------------|------------|----------------|------------|----------------|------------|
| Co | 61.78 | C | 0.23 | Al | 0.01 |
| Cr | 29.6 | Fe | 0.23 | Ti | 0.01 |
| Mo | 6.4 | Ni | 0.2 | B | 0.007 |
| Mn | 0.8 | N | 0.17 | P | 0.003 |
| Si | 0.7 | O | 0.0161 | Si | 0.001 |

The LENS® machine gives a high degree of control over most deposition aspects. These include laser power, powder flow rate, laser on traverse speed, laser off traverse speed, hatch spacing, hatch shrink, and hatch direction. This study varied some of the key parameters which affect microstructure.

Several LENS® machine parameters remained constant during all tests in this study. A measured laser power of 285W and hatch size and shrink of 0.015 inches were held constant for every deposition. Powder flow rates were verified before each set of tests by taking a weight measurement of the powder ejected for a given time period.

As mentioned by Bontha, material cooling rate determines the microstructure (Bontha and Klingbeil 2003), which in turn controls material properties, including hardness. The settings varied in these experiments were chosen due to their effect on cooling rates. The varied parameters were: 1. Laser Traverse Speed, 2. Powder Feed Rate, and 3. Layer Build Height.

After deposition, to prepare specimens for optical viewing, polishing to a smoothness of 0.3 microns and etching with either electrolytic etching in a 5% HCl solution or a 92% HCl / 5% H₂SO₄ / 3 % HNO₃ was performed. It was observed that the deposited microstructures were

more difficult to etch than the wrought microstructures, which might indicate that the deposited microstructures are more resistant to corrosion.

The goals of Phase 1 consisted of two parts. First, to verify that powdered Biodur CCM+ CoCrMo alloy would adhere to a substrate of the same alloy using the LENS® process. Second, if adherence occurred, to test a broad range of LENS® parameters to gain insight on how each LENS® parameter would affect the deposited structure. From previous experiments with Ti-6Al-4V, LENS® produced both columnar and equiaxed, fine grain structures (Kobryn et al. 2000). Since CoCrMo has a higher thermal conductivity than Ti-6Al-4V, the microstructure was expected to be a finer, equiaxed structure than those resulting from Ti-6Al-4V (Hofmeister et al. 2001).

For Phase 1, a wide range of LENS® parameters were chosen and a full factorial test organized randomly was performed with no replicates. The varied parameters are shown in Table 2. Both sides of each 2.25” diameter disk were used for the experiments. Figure 1 illustrates the layout of the depositions and the cross-sectioning used to view microstructures and test cross-sectional hardness. Each deposit was designed to be 0.5”x 0.25” x 6 layers thick.

Table 2. LENS® parameters used in Phase 1

| | |
|--------------------------------------|--------------------|
| Laser Traverse Speed (in/min) | 15, 20, 25, 30, 35 |
| Powder Feed Rate (g/min) | 0.26, 0.43, 0.57 |
| Layer Build Height (in) | 0.01, 0.02 |

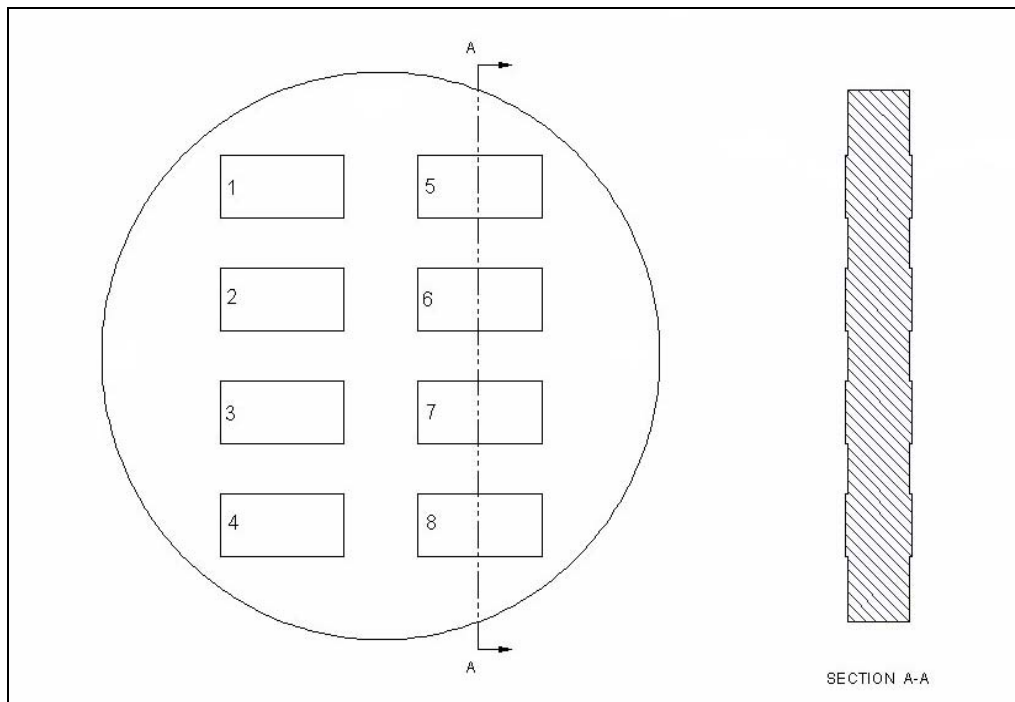


Figure 1. Arrangement of LENS® depositions and cross-sectioning location.

With the results of the first phase showing that Biodur CCM+ could be deposited by LENS® processing, Phase 2 was used as a replicate to verify that consistent microstructure and hardness results could be obtained when using identical LENS® settings.

From the results of the first phase, the field was reduced to 16 parameter sets considered to be non-porous based on observed microstructures and that demonstrated the highest hardness values. After randomizing, the depositions were performed as shown in Table 3.

Table 3. LENS® parameters for each deposition in Phase 2

| Deposition Number | Laser Traverse Speed (in/min) | Powder Feed Rate(g/min) | Layer Build Height (in) |
|--------------------------|--------------------------------------|--------------------------------|--------------------------------|
| 1 | 25 | 0.43 | 0.01 |
| 2 | 30 | 0.57 | 0.01 |
| 3 | 25 | 0.26 | 0.01 |
| 4 | 15 | 0.26 | 0.01 |
| 5 | 30 | 0.43 | 0.02 |
| 6 | 20 | 0.43 | 0.01 |
| 7 | 20 | 0.26 | 0.02 |
| 8 | 25 | 0.57 | 0.02 |
| 9 | 35 | 0.26 | 0.02 |
| 10 | 35 | 0.57 | 0.02 |
| 11 | 25 | 0.26 | 0.02 |
| 12 | 35 | 0.43 | 0.02 |
| 13 | 20 | 0.26 | 0.01 |
| 14 | 30 | 0.57 | 0.02 |
| 15 | 25 | 0.43 | 0.02 |
| 16 | 30 | 0.26 | 0.01 |

The prime importance of wear resistance in orthopedic bearing surfaces led to the experiments of Phase 3. This phase attempted to qualify the abrasive wear resistance of 6 depositions that consistently had the highest hardness values from the previous two phases. The parameters used are given in Table 4. The tests consisted of two repetitions for each of the six LENS® deposition parameters; one for hardness and microstructure testing and one for wear testing. These were significantly larger than the previous depositions due to the need for a greater surface area required by the wear test. The deposition pattern was designed to create a 1.0”x 2.0”x 0.25” deposition onto each 2.25-inch diameter disk, which was approximately 32 times the volume of the depositions in Phases 1 and 2. The specimens were cut using a wire EDM as shown in Figure 2. ASTM G65-94, entitled “Standard test for measuring abrasion using the dry sand/rubber wheel apparatus,” prescribed the method of wear testing. This test allows free-falling abrasive sand to fall between a rotating rubber wheel and the specimen being pressed against it (Figure 3).

Table 4. LENS® parameters for each deposition in Phase 3

| Deposition Number | Laser Traverse Speed (in/min) | Powder Feed Rate(g/min) | Layer Build Height (in) |
|-------------------|-------------------------------|-------------------------|-------------------------|
| 1 | 20 | 0.26 | 0.01 |
| 2 | 25 | 0.26 | 0.02 |
| 3 | 30 | 0.26 | 0.01 |
| 4 | 30 | 0.57 | 0.01 |
| 5 | 35 | 0.26 | 0.02 |
| 6 | 25 | 0.43 | 0.01 |

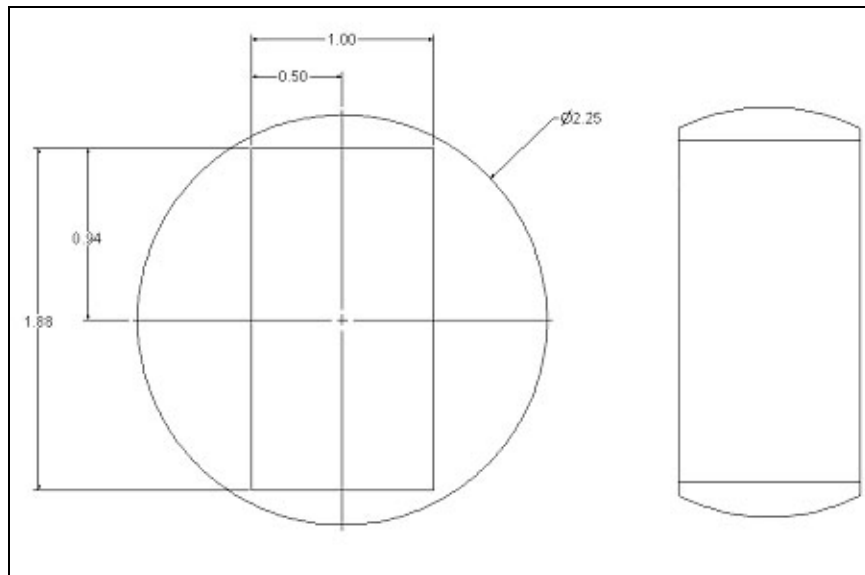


Figure 2. Arrangement of Phase 3 LENS® depositions shown before and after EDM processing.

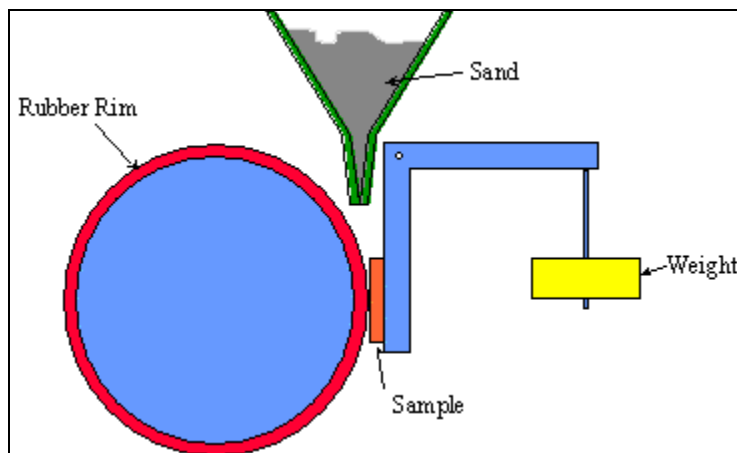


Figure 3. Demonstration of the wear test per ASTM G65-94.

RESULTS

Observation showed a lack of adhesion or porosity in some of the deposited material. Observable porosity occurred when insufficient applied energy left the incoming powder unmelted (for example, a deposit when coupling fast laser traverse speeds with high powder feed rates). Porous depositions turned out to have a softer average hardness than the average hardness of non-porous depositions. In cases of well-adhered deposited material, the measured Vickers hardness equaled or exceeded the unheated base material. Of the 30 total Phase 1 depositions, the 12 softest depositions had some observable porosity while the remaining 18 depositions contained only one with visible porosity.

The LENS® process thermally affects the base material substrate during deposition. The continual incident energy from the laser caused heating that slightly changed the hardness properties. The measured average hardness for an unheated base was 40.7 Rockwell C and the average hardness for the base material after depositions was 37.8. Phase 1 LENS®-deposited CoCrMo ranged from a low of 43 to a high of 49 on the Rockwell C scale.

The interface between deposited structure and base material showed a highly localized heat affected zone (HAZ). The interface demonstrated good adherence and no visible porosity. In addition, the deposited microstructure was significantly refined when compared with the wrought microstructure. These comparisons are shown in Figure 4.

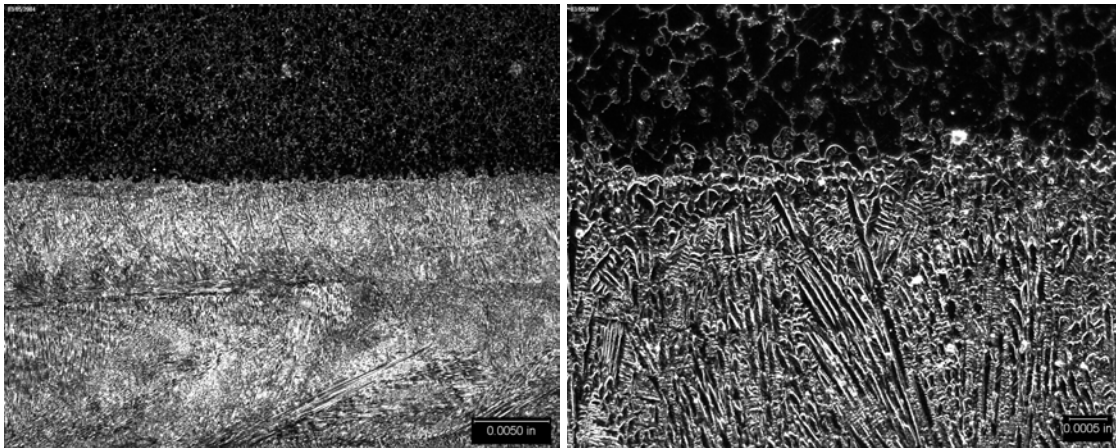


Figure 4. Micrograph of a typical interface between the LENS® deposition and base material (20x objective lens left and 50x right). The base material is shown above the deposit.

A higher magnification view of deposit cross-sections showed three types of grains in the typical LENS®-deposited CoCrMo: 1) fine, equiaxed grains, 2) slightly more coarse, equiaxed grains, and 3) columnar or dendritic grains (Figure 5). While observation showed all types of grain structures in the deposited material, they were more common in certain areas. Fine grains dominated in the last deposited layer. Columnar grains were observed to form in the direction of the laser traverse at layer interfaces. The coarse equiaxed grains were present in layers closer to the base of the deposit due to grain growth associated with the reheating effect that additional layers deposited on top of previous layers.

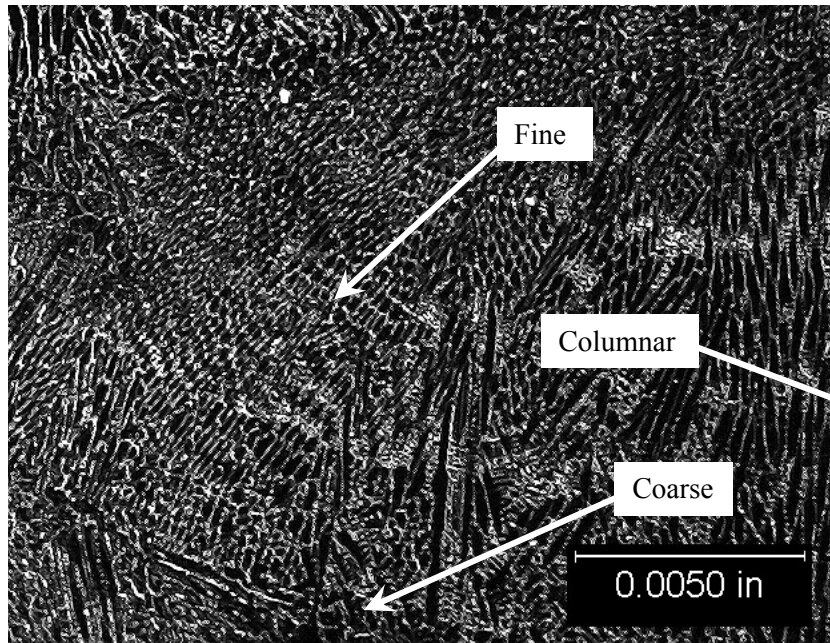


Figure 5. Micrographs of typical base and deposited grain structures (50x).

In Phase 2, only the 16 hardest deposition parameters were examined to verify the results from Phase 1. Testing showed the hardness values of depositions within the same range as Phase 1 values, with one exception where the measured hardness varied by 15.9% from the value measured in Phase 1. All other depositions fell within a maximum 6.4% and a mean 3.5% variation from the measured hardness values in Phase 1 (Table 5).

Table 5. Comparison of measured Vickers hardness values of Phase 1 and Phase 2 depositions

| Phase 1 Hardness | Phase 2 Hardness | % Difference |
|------------------|------------------|--------------|
| 457 | 436 | -4.6% |
| 459 | 439 | -4.2% |
| 460 | 453 | -1.6% |
| 461 | 468 | 1.5% |
| 461 | 465 | 0.7% |
| 465 | 460 | -1.2% |
| 467 | 471 | 0.9% |
| 468 | 450 | -3.8% |
| 472 | 442 | -6.4% |
| 473 | 479 | 1.3% |
| 476 | 501 | 5.4% |
| 476 | 473 | -0.7% |
| 477 | 469 | -1.8% |
| 478 | 472 | -1.2% |
| 494 | 470 | -4.8% |
| 513 | 431 | -15.9% |

Further Examination showed much smaller carbide formations in deposited structures than those in the base material. Higher magnification micrographs confirmed that carbides formed at the grain boundaries (Figure 6).

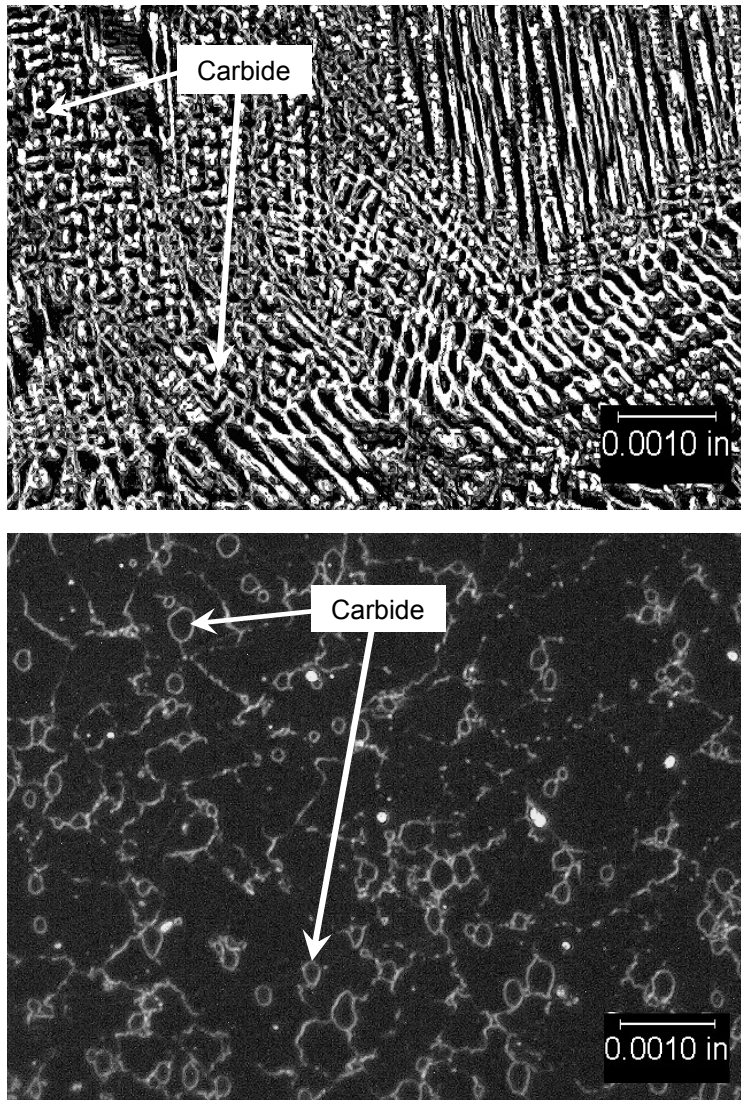


Figure 6. Micrographs showing carbides in LENS®-deposited (top) and wrought material (bottom).

Phase 3 hardness values consistently measured lower than those of Phases 1 and 2. Rockwell C hardness measurements were performed on the top surface and on cross-sections. These values measured about 15% lower than the hardness tests performed on smaller depositions. Observation showed a decrease in hardness in every deposition from Phase 3.

The large size of the depositions allowed for polishing and etching of the top surfaces. Top surface polishing and etching of depositions for Phase 1 and Phase 2 was not possible due to the deposition arrangement. As expected, top surface Phase 3 microstructures appeared equiaxed, whereas cross-sectional views showed columnar grains in larger volume fractions due to the lower cooling rates inherent with larger depositions (Figure 7).

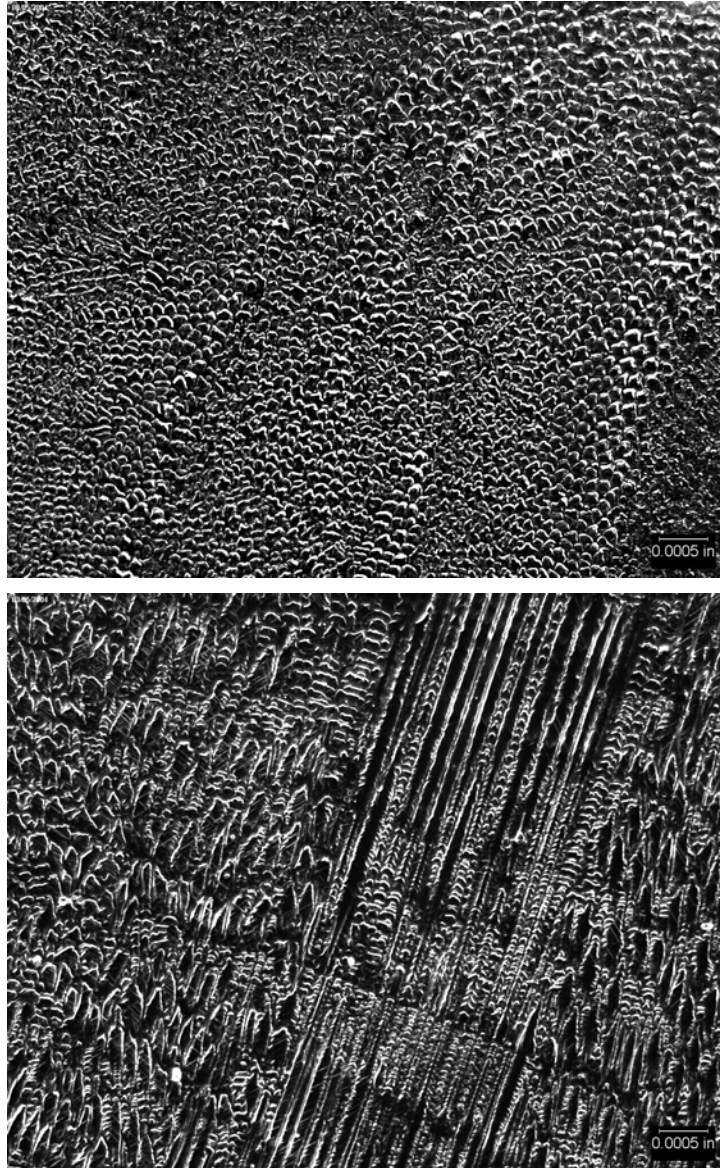


Figure 7. Micrographs of typical top (above) and side (below) views of a LENS®-deposited material.

Wear results, per the ASTM G65 standard, measured weight loss and calculated the volumetric loss after abrasive wear testing. Wear loss proved 2.4 times greater for deposited material compared to the base material. The testing showed negligible difference in wear from one deposited part to another.

DISCUSSION

LENS®-deposited CoCrMo consistently forms a fine grain structure compared to the wrought version of the alloy. This occurs as a result of the rapid quenching inherent with LENS®-deposited alloys. Since LENS® creates a very small molten pool, the entire substrate can act as a heat sink, dissipating the energy and rapidly quenching the melt pool.

The rapid quenching of the molten alloy causes small carbide formations within LENS®-deposited CoCrMo. This rapid quenching does not allow sufficient time for large carbides to precipitate. Although observation showed carbides on the grain boundaries, SEM analysis would be necessary to fully verify the location of carbide formation within the LENS®-deposited alloy.

Porosity can occur within the deposition if the incident energy from the LENS® laser does not completely melt the substrate and the injected powder. The lack of melting creates “bridges” of unmelted material and air pockets. The lack of material within the structure can reduce the hardness of the deposition. Proper combinations of powder feed rate and laser traverse speed/laser power can be chosen to mitigate this problem.

LENS®-deposited material proved harder than wrought material for the smaller depositions. Grain refinement produced this increase by increasing the number of grain boundaries. The grain boundaries in turn resist dislocation motion under stress.

The measured hardness for large depositions proved softer than that of the smaller depositions. Grain growth and porosity often occur in large deposits (Kobryn and Semiatin 2001) and could help explain this.

The wrought alloy used for the substrate was softened when heated during the LENS® process. The releasing of stored strain energy in the wrought material due to dislocation motion at elevated temperatures was most likely the basis for this.

Deposited CoCrMo showed greater wear rates than the base material under the ASTM G65-94 abrasive wear test. Other researchers have determined that carbide hardness and volume fraction are the main contributors to the wear resistance of cobalt-based alloys (Atamert and Stekly 1993). Wrought material has much larger carbide formations than those of LENS®-deposited material. The decrease in carbide size found in LENS®-deposited CoCrMo may reduce the armoring effect that the large carbides in the wrought alloy provide. This can lead to direct carbide removal as the abrasive particles easily penetrate the matrix of the LENS®-deposited CoCrMo, translating to lower wear resistance when subjected to this specific abrasion test (Atamert and Stekly 1993; Schmidt et al. 1996).

Orthopedic bearing surfaces suffer from adhesive and abrasive wear. This can result in direct material removal or in the formation of microcracks with subsequent wear particle production through microfracture. A high resistance against adhesive and abrasive wear is usually provided by materials with high hardness and high fracture toughness, respectively. Metal matrices commonly provide for high fracture toughness, while carbides are effective for increasing the material hardness (Schmidt et al. 1996). Although the LENS®-deposited CoCrMo demonstrated higher hardness, there was a decrease in carbide size. The decrease in carbide size is believed to be the cause of the demonstrated lower abrasive wear during the abrasive wear test. It is unclear whether this will lead to less wear resistance in an orthopedic bearing surface application, or whether the smaller, dispersed carbides combined with the higher hardness values will provide for improved resistance to wear in like-on-like metal abrasion, which may have different wear phenomena.

CONCLUSIONS AND FUTURE WORK

These tests prove that it is possible to deposit powdered CoCrMo onto wrought CoCrMo via LENS®. Based on microstructure observation and hardness tests, LENS® can create a refined grain structure that translates into a slightly harder material when depositing a volume of material significantly smaller than the substrate. As the deposit size increases, the hardness lessens. Testing per ASTM G65 shows that the abrasive wear of deposited CoCrMo is about 2.4

times greater than that of the wrought version of the alloy. The decrease in carbide size within the part as a result of rapid solidification inherent in the LENS® process likely causes this reduction in resistance to gouging by dry sand particles.

Although this experiment proves the feasibility of depositing powdered CoCrMo onto ASTM F1537 CoCrMo, further experimentation would be required to establish the properties required to use LENS®-deposited CoCrMo in implant bearing surface applications, especially for metal-on-metal bearing surfaces.

REFERENCES

- Amstutz, H. C., P. Campbell, N. Kossovsky, and I. C. Clarke. 1992. Mechanisms and clinical significance of wear debris-induced osteolysis. *Clinical Orthopaedics* 276: 7-18.
- Atamert, S., and J. Stekly. 1993. Microstructure, wear resistance, and stability of cobalt based and alternative iron based hardfacing alloys. *Surface Engineering* 9, no. 3 (March): 231-240.
- Bontha, S., and N.W. Klingbeil. 2003. Thermal process maps for controlling microstructure in laser-based solid freeform fabrication. *Solid Freeform Fabrication Proceedings*. August 4-6, 2003 by The University of Texas at Austin.
- Brice, C. A., K. I. Schwendner, D. W. Mahaffey, E. H. Moore, and H. L. Fraser. 1999. Process variable effects on laser deposited Ti-6Al-4V. *Solid Freeform Fabrication Proceedings*, edited by D. L. Bourell, J. J. Beaman, R. H. Crawford, H. L. Marcus, and J. W. Barlow. August 9-11, 1999 by The University of Texas at Austin.
- Hamilton, H. W., and J. Gorczyca. 1995. Low friction arthroplasty at 10 to 20 years-consequences of plastic wear. *Clinical Orthopaedics* 311: 3-20.
- Hofmeister, W., M. Griffith, M. Ensz, and J. Smugeresky. 2001. Solidification in direct metal deposition by LENS processing. *Journal of Materials* (September): 30-34.
- Kobryn, P.A., E. H. Moore, and S. L. Semiatin. 2000. The effect of laser power and traverse speed on microstructure, porosity, and build height in laser-deposited Ti-6Al-4V. *Scripta Materialia* 43: 299-305.
- Kobryn, P. A., and S. L. Semiatin. 2001. Mechanical properties of laser-deposited Ti-6Al-4V. *Solid Freeform Fabrication Proceedings*, edited by D. L. Bourell, J. J. Beaman, R. H. Crawford, H. L. Marcus, J. W. Barlow, and K. L. Wood. August 6-8, 2001 by The University of Texas at Austin.
- Medley, J.B., F. W. Chan, J. Jan, and D. Boby. 1996. Comparison of alloys and designs in a hip simulator study of metal on metal implants. *Clinical Orthopaedics* 329S: S148-S159.
- Ratner, B. D., A. S. Hoffman, F. J. Schoen, J. E. Lemons. 1996. *Biomaterials Science: An Introduction to Materials in Medicine*. San Diego: Academic Press.
- Schmalzried, T. P., E. D. Szuszczewicz, K. H. Akizuki, K. H. Peterson, and H. C. Amstutz. 1996. Factors correlating with long term survival of McKee-Farrar total hip prosthesis. *Clinical Orthopaedics* 329S: S48-S59.
- Schmidt, M., H. Weber, and R. Schön. 1996. Cobalt chromium molybdenum metal combination for modular hip prostheses. *Clinical Orthopaedics* 329S: S35-S47.

Steen, W. M. 1985. Surface engineering with a laser. *Metals and Materials* 1, no. 12 (Dec): 730-736.

Walker, P. S., and B.L. Gold. 1971. The tribology (friction, lubrication, and wear) of all-metal artificial hip joints. *Wear* 17: 285-299.